Notes

Proton Nuclear Magnetic Resonance Study of Water in Flocs

A. Fan, P. Somasundaran,* and N. J. Turro

Langmuir Center for Colloids and Interfaces, Columbia University, New York, New York 10027

Received January 15, 1998. In Final Form: April 7, 1999

Introduction

Polymer/surfactant adsorption can lead to colloidal stability or particle flocculation, both of which are of importance in many industrial processes. Floc structure is one of the most important features of particle flocculation and this involves floc size, density and strength.[1−6] Spectroscopic techniques to investigate floc structure have been mainly limited to small-angle neutron scattering (SANS)[7−9] and CAT scan.[10] SANS is based on the assumption that the observed interference pattern of the scattered radiation is determined by the distribution of separations between particle centers in the flocs.[6] CAT is a special X-ray instrument that can produce three-dimensional images of an object. Although designed for medical purposes, the CAT has been effectively utilized to study sedimentation and flocculation systems.[10] In addition to SANS and CAT scan, computer simulation has also been used to characterize floc structure.[11−15] The purpose of this work is to show the potential of using proton nuclear magnetic resonance (NMR) to study water in flocs, and thereby obtain information on floc structure by analysis of NMR line shapes, intensities, and signal positions.

Proton NMR of water has been applied extensively to the study of solid−solute interactions such as water−glass,[16−18] water−clay,[19,20] protein solution,[21] biological tissues,[22] water−hydrated alumina,[23] and water−silica powder.[24] A marked decrease of the proton longitudinal and transverse relaxation times, T_1 and T_2, as well as an increase in the T_1/T_2 ratio has been observed compared to the values for pure or "bulk" water. The results were interpreted in terms of layers of water molecules with restricted mobility in the vicinity of an interface. Water molecules are dynamically exchanged between an environment in which they relax slowly (free-water phase) and one in which they relax rapidly (bound-water phase at or near the interface). Under conditions of rapid exchange on the NMR time scale, a single relaxation rate is observed and is the weighted average of the individual rate for each environment.[25] Accordingly, the signal on the spectrum is broader for a higher ratio of bound to free water.

When the exchange of molecules between sites corresponding to different resonances is slow on the NMR time scale, multiple peaks can be observed. Two signals were reported for ion-exchange resin−water[26] and silica−water systems.[27] One signal was attributed to bulk water, while the other signal corresponds to water inside the resin or silica pores. Similar phenomena were observed for protein−water[28,29] and carbosil−water[30] systems and a series of gels and macroreticular ion-exchange resins in water.[31,32]

The difference in the chemical shifts of the water signals has been discussed in terms of the number of hydrogen bondings for oxide particles (silica systems) and ion-hydration effect (resins). However, this concept was challenged when multiple signals were found for systems without either donor−acceptor interactions or the ion-hydration effect. The chemical shift difference for water signals was proposed to result from the contact of water with solids.[33] It was also found that signals with different chemical shift values resulted when different pore sizes were employed.

In our investigation of alumina and zeolite flocs, the "H-bonding giving rise to the shift" was shown to be inadequate to explain the observations. When alumina and zeolites were studied in this investigation, in addition to the signal due to bulk water, an extra downfield-shifted signal was also observed. This second signal could not be adequately accounted for using the hydrogen-bonding theory, and hence it is attributed to the bulk magnetic

(1) Glasgow, L. A. *Chem. Eng. Prog.* **1989**, *85* (8), 51.
(2) Klimpel, R. C.; Hogg, R. *J. Colloid Interface Sci.* **1986**, *113*, 121.
(3) Tambo, N.; Watanabe, Y. *Water Res.* **1979**, *13*, 409.
(4) Mougil, B. M.; Vasudevan, T. V. *Miner. Metall. Process.* **1989**, *6*, 142.
(5) Bache, D. H.; Al-Ami, S. H. *Water Sci. Technol.* **1989**, *21*, 529.
(6) Dickinson, E.; Eriksson, L. *Adv. Colloid Interface Sci.* **1991**, *34*, 1.
(7) Wong, K.; Cabane, B.; Duplessix, R. *J. Colloid Interface Sci.* **1988**, *123*, 466.
(8) Wong, K.; Cabane, B.; Somasundaran, P. *Colloids Surf.* **1988**, *30*, 355.
(9) Cabane, B.; Wong, K.; Wang, T. K.; Lafuma, F.; Duplessix, R. *Colloid Polym. Sci.* **1988**, *266*, 101.
(10) Somasundaran, P.; Huang, Y. B.; Gryte, C. C. *Powder Technol.* **1987**, *53*, 73.
(11) Dickinson, E. *Colloids Surf.* **1989**, *39*, 143.
(12) Dickinson, E. *J. Colloid Interface Sci.* **1987**, *118*, 286.
(13) Ansell, G. C.; Dickinson, E. *Faraday Discuss. Chem. Soc.* **1987**, *83*, 167; *J. Chem. Phys.* **1986**, *85*, 4079; *Phys. Rev.* **1987**, *35A*, 2349.
(14) Nagatani, T. *Phys. Rev.* **1989**, *40A*, 7286.
(15) Yuang, Y. B.; Somasundaran, P. *Phys. Rev.* **1987**, *36A*, 4518.
(16) Glasel, J. A.; Lee, K. H. *J. Am. Chem. Soc.* **1974**, *96*, 970.
(17) Fung, B. M.; McGaughy, T. W. *J. Magn. Reson.* **1981**, *43*, 316.
(18) Hirama, Y.; Takahashi, T.; Hino, M.; Sato, T. *J. Colloid Interface Sci.* **1996**, *184*, 349.
(19) Woessner, D. E. *J. Magn. Reson.* **1980**, *39*, 297.
(20) Delville, A.; Letellier, M. *Langmuir* **1995**, *11*, 1361.
(21) Koenig, S. H.; Bryant, R. G.; Hallenga, K.; Jacob, G. S. *Biochemistry* **1978**, *17*, 4348.
(22) Finch, E. D.; Homer, L. D. *Biophys. J.* **1974**, *14*, 907.
(23) (a) Pearson, R. M. *J. Catal.* **1971**, *23*, 388. (b) Baker, B. R.; Pearson, R. M. *J. Catal.* **1974**, *33*, 265.
(24) Hanus, F.; Gillis, P. *J. Magn. Reson.* **1984**, *59*, 437.
(25) Zimmerman, J. R.; Brittin, W. E. *J. Phys. Chem.* **1957**, *61*, 1328.
(26) Gordon, J. E. *J. Phys. Chem.* **1962**, *66*, 1150.
(27) Clifford, J.; Pethica, B. A. *Hydrogen-Bonded Solvent Systems*; Taylor & Francis: London, 1968; p 169.
(28) Berendsen, H. J. C.; Migchelsen, C. *Ann. N. Y. Acad. Sci.* **1965**, *125*, 365.
(29) Clifford, J.; Sheard, B. *Biopolymers* **1966**, *4*, 1057.
(30) Turov, V. V.; Leboda, R.; Bogillo, V. I.; Skubiszewska-Zieba, J. *Langmuir* **1997**, *13*, 1237.
(31) Frankel, L. S. *J. Phys. Chem.* **1971**, *75*, 1211.
(32) (a) Creekmore, R. W.; Reilly, C. N. *Anal. Chem.* **1970**, *42*, 570; *Anal. Chem.* **1970**, *42*, 725.
(33) Drago, R. S.; Ferris, D. C.; Burns, D. S. *J. Am. Chem. Soc.* **1995**, *117*, 6914.

10.1021/la980068g CCC: $18.00
Published on Web 06/18/1999

susceptibility (BMS)[34,35] effect. The basic idea in the BMS theory is that a water molecule inside and outside a compartment will possess two different chemical shift values. This effect was found to be important in an in vivo NMR imaging study of biological tissues[33,34] and may be useful for explaining what was observed in this study. According to BMS theory, the downfield shift results from water trapped in small compartments: pores in the particles or microchannels within the flocs depending on what kind of particles are used.

Experimental Section

Materials. Alumina powder (Praxair Surface Technologies) used had an average size of 0.3 μm and a BET surface area of approximately 15 m^2/g, and they aggregate into 20-μm microflocs in water as measured by Microtrak (Leeds & Northrup Instruments). Zeolite particles of different crystal sizes were synthesized[36] and had a pore size on the order of 5 Å and a cylindrical pore structure; 10 and 20-μm zeolite particles possess a Si/Al ratio of 80/20 (16 m^2/g), and 100-μm particles of silicalite (5 m^2/g) were employed. Poly(acrylic acid) (PAA) of molecular weight 10 000 was obtained from Polysciences Inc. Cationic copolymer Percol (Allied Colloids Inc.) was a copolymer of acrylamide and dimethyl aminoethyl acrylate of equal fraction, the latter being fully quaternized and therefore positively charged over a wide pH range. All the samples were prepared with 0.1 N NaCl solutions. Triply distilled water was used throughout the experiment.

Flocculation Test. The method for dual polymer flocculation was the same as that described before.[39] The supernatant turbidity was read with a turbidimeter (HF scientific Inc.), and the sediment was transferred to a cylindrical volumetric tube for the sediment volume measurement.

NMR Measurements. Flocs produced from flocculation tests were carefully transferred into a standard 5-mm NMR tube and allowed to settle for a certain amount of time (the typical time scale is a few hours of settling time). The tube was filled so that the solid filled the volume of the probe coil. The ^{1}H NMR spectrum was obtained using a VXR Varian-400-MHz NMR spectrometer. Spectra were obtained at 25 °C. In all spectra, 64 scans were acquired without spinning. For all sets of measurements, floc preparation and NMR measurement were made on a parallel time scale, which ensured the same settling time for flocs in each sample.

Results and Discussion

1. NMR spectra of Native Flocs. With many of the samples investigated, separate resonances for the water protons were observed for alumina−water and zeolite−water systems, indicating a slow exchange of molecules between the sites corresponding to these resonances on the NMR time scale. These separate signals were attributed to water in microchannels (trapped water) and macrochannels (bulk water) of the flocs as shown in Figure 1. In the case of highly porous zeolite, the porous internal surface within individual particles forms microchannels in which the water is adsorbed; while for alumina, the microchannels exist within the alumina aggregates formed by numerous primary alumina particles. In contrast to previous NMR reports on colloidal systems described above, our research involves in situ study of natural flocs

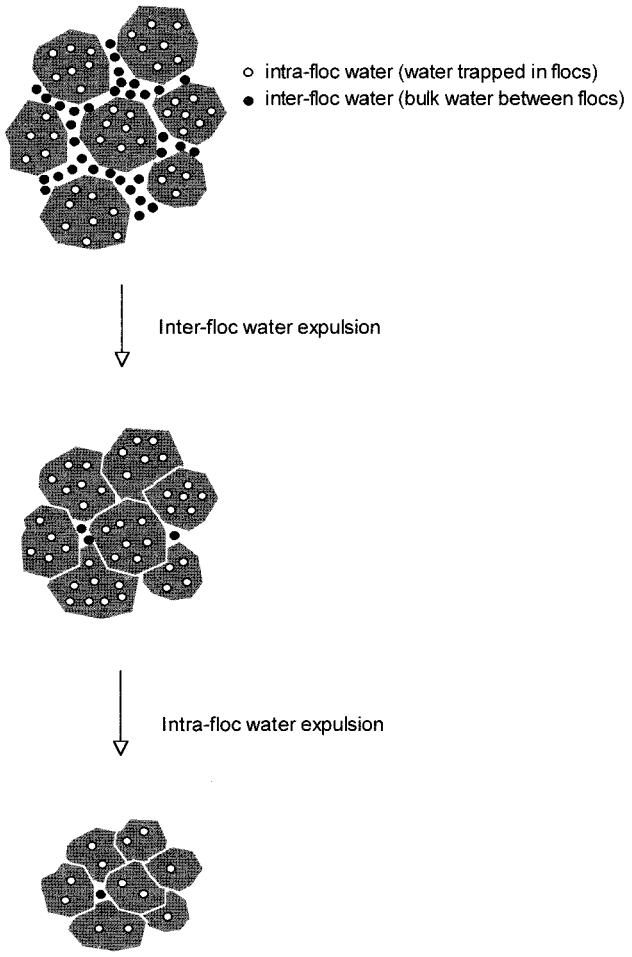

Figure 1. Schematic representation of intrafloc water and interfloc water and their explusion processes.

where the solid−liquid ratio is not quantitatively manipulated. It was proposed[37] that two processes of water removal can occur with time: relatively fast expulsion of water in the macrochannels (bulk water removal) and relatively slow expulsion of water from within the flocs (trapped water removal). The former is an interfloc process while the latter is an intrafloc one (Figure 1). Therefore, when ratios of different water signals are examined, the values are for different settling times of the flocs because water is extruded as the floc densifies. Only flocs settled for the same time can be compared with each other. The time effect for a zeolite−water system is shown in Figure 2, where the peak for trapped water increases with time as the zeolite floc settles and densifies due to bulk water expulsion.

Common flocculants are of three types: salt, polymer, and surfactant. Salt and small polymer molecules are expected to induce flocculation mainly by charge neutralization, which produces very compact and dense flocs. In contrast, bridging is considered to be the mechanism for large polymer-induced flocculation, and the resulting flocs are much bigger and less dense than those produced by salt or small polymers. Surfactants are less commonly used as flocculants. Surfactants induce flocculation by imparting hydrophobicity to the particles when the surfactant species orients with its hydrocarbon moiety toward the aqueous phase.[38] Examples of the proton NMR of a compact and a loose floc system are shown in Figure 3. On one hand, since the fraction of trapped water is related to the floc density, loose flocs produced by the addition of small amounts of PAA contain an amount of

(34) Chu, S. C.-K.; Xu, Y.; Balschi, J. A.; Springer, C. S., Jr. *Magn. Reson. in Medicine*; Academic Press: San Diego, CA, **1990**; Vol. 13, p 239.
(35) Springer, C. S., Jr. In *NMR in Physiology and Biomedicine*; Academic Press: San Diego, CA, 1994; Chapter 5.
(36) Zhao, D.; Qiu, S.; Pang, W. *Zeolites* **1993**, *13*, 478.
(37) Harris, C. C.; Somasundaran, P.; Jensen, R. R. *Powder Technol.* **1975**, *11*, 75.
(38) Somasundaran, P.; Healy, T. W.; Fuerstenau, D. W. *J. Colloid Interface Sci.* **1966**, *22*, 599.
(39) Somasundaran, P.; Fuerstenau, D. W. *J. Phys. Chem.* **1966**, *70*, 90.

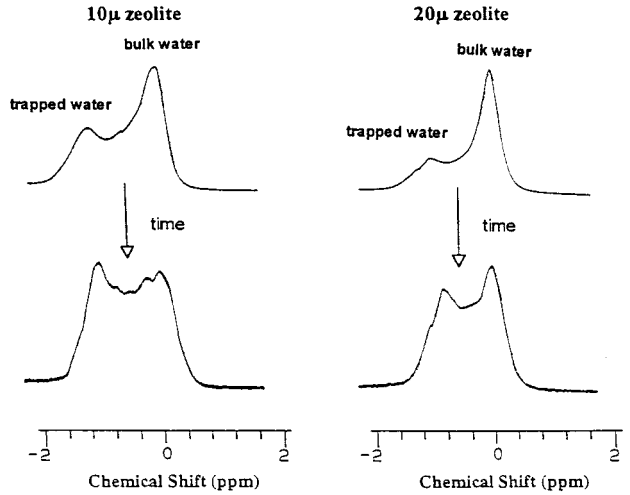

Figure 2. Time effect on NMR peak ratio.

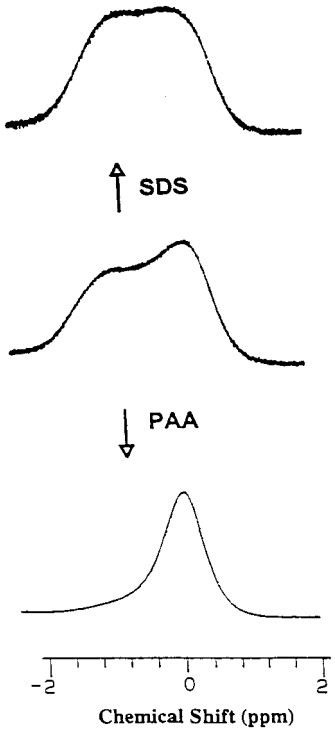

Figure 3. Flocs produced by three kinds of flocculants: salt, polymer, and surfactant.

trapped water that is so small that only one bulk water peak is observed; on the other hand, the addition of appropriate amounts of sodium dodecyl sulfate (SDS) enhances the floc packing density.

For a fixed time scale, the particle size can be expected to affect the packing. Figure 4 shows the NMR spectra for zeolite−water systems with particle sizes varying by a factor of 10. It can be seen that the peak ratio of the trapped water to bulk water increases with decreasing particle size, indicating a denser packing of smaller particles and a greater fraction of trapped water for two ZSM-5 zeolites differing in particle size but not in pore size or polarity. The three kinds of zeolite particles possess the same internal pore size and pore structure, thus, in agreement with BMS theory, result in the same frequency shift for the trapped water. It is important to note that the composition of the 100-μm silicalite particles (Si:Al > 1000) is different from those of the other two (Si:Al = 80:20). Nevertheless, the downfield shifts of water signals are

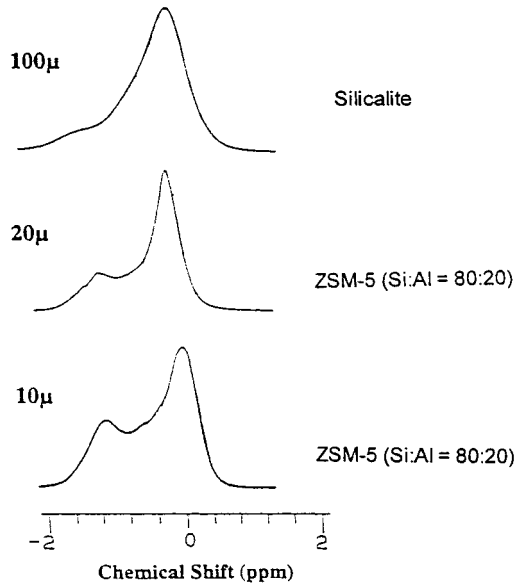

Figure 4. Particle size effect for zeolite in water.

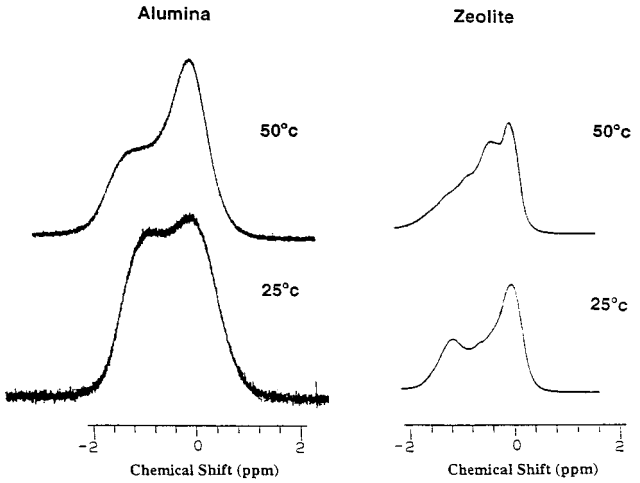

Figure 5. Temperature effect for alumina and zeolite flocs.

very similar for all of the zeolite samples. This again indicates a compartmental effect instead of donor−acceptor interaction with the particle surface.

Packing density can be changed also with temperature. This effect can be seen from an examination of Figure 5. For hydrophilic alumina particles, the trapped water peak decreases markedly with an increase in temperature, which means that the packing is less dense at higher temperature. For 10-μm zeolite (Si:Al = 80:20) which is much less hydrophilic than alumina, however, the temperature effect is quite different. The trapped water peak, instead of decreasing without changing its original resonance frequency, moves toward the bulk water peak as temperature is increased. This is associated with the fact that water molecules are expelled from the small hydrophobic pores as the temperature is raised, and/or exchange between water inside and outside the pores begins to take place.

2. Surfactant-Induced Flocs. The adsorption of sodium dodecyl sulfate (SDS) on alumina has been well-studied, with an adsorption isotherm which can be divided into four regions[39] (Figure 6). The surfactant adsorbs noncooperatively and electrostatically as individual ions in region I and associate into solloids (hemimicelles) in region II of the isotherm. In the solloids, the surfactants are oriented with their charged headgroups toward the

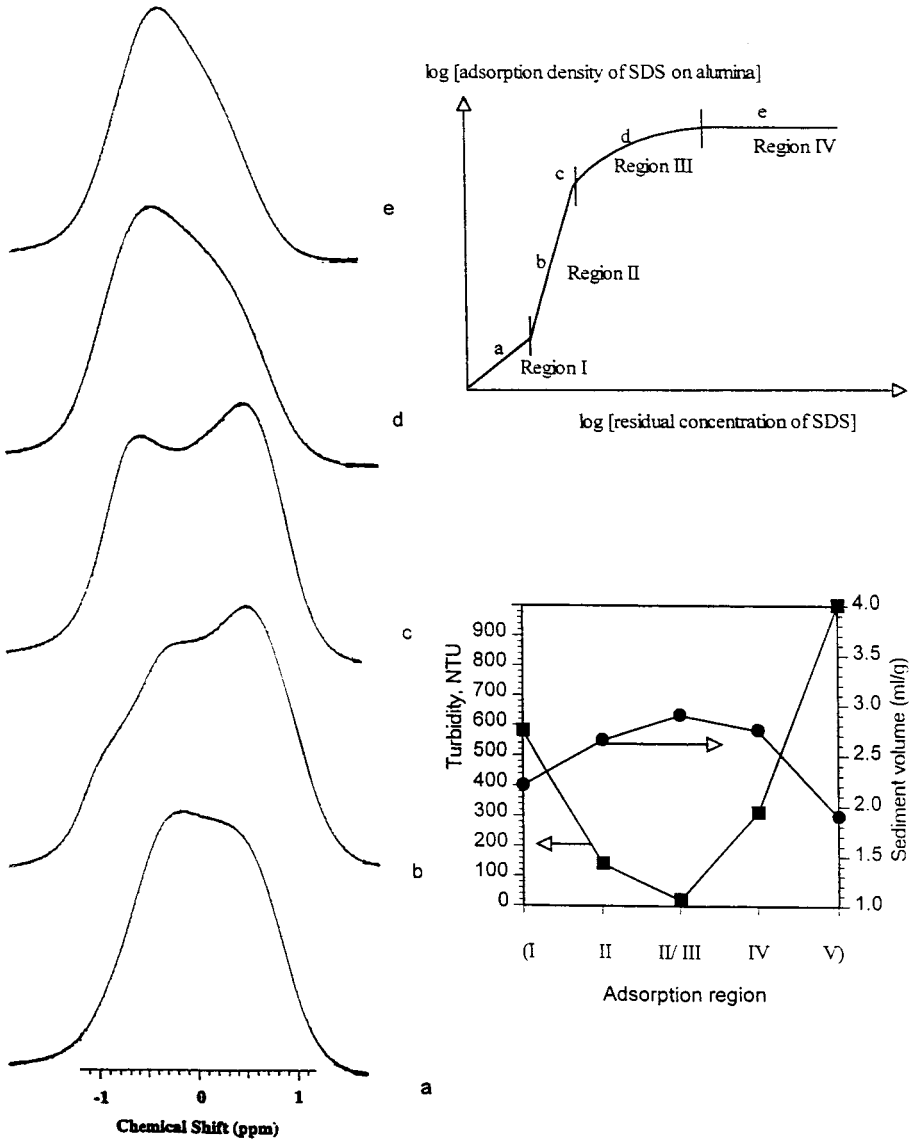

Figure 6. SDS-induced flocs at different SDS concentrations (left, NMR spectra; upper right, adsorption isotherm; lower right, flocculation results).

solid surface, while the hydrocarbon chains protrude into the aqueous phase, thus forming hydrophobic patches on the surface. Further adsorption results in an increasing number of surfactant aggregates, with surfactant molecules adsorbing with an opposite orientation once the surface is neutralized by the oppositely charged surfactant. Finally, in the plateau region, region IV, the adsorption layer possesses the structure of a bilayer with the adsorbed surfactant presenting the external surface with a changed structure.

Figure 6 shows the water signals measured for alumina flocs with different coverages of SDS. The flocculation data could be correlated with the NMR spectra. The SDS coverage is illustrated by indicating its position on the corresponding adsorption isotherm. As described above, the hydrophobicity of alumina increases with SDS adsorption in adsorption regions I and II and starts to decrease from region III until it reaches a constant value in region IV where adsorption is saturated. Therefore, particles in sample c are most hydrophobic and have the strongest tendency for flocculation (Figure 6). Accordingly, the separation between the two peaks varies and shows a clear trend. The separation for sample c is the largest and decreases toward the two ends of the adsorption isotherm. This change in peak separation indicates a change of the compartmental structure in the flocs. A more downfield-shifted peak denotes better screened and smaller compartments for trapped water. As the compartmental structure becomes bigger and more open, the two peaks start to approach each other.

The more hydrophobic the particles are, the stronger can be their tendency to aggregate in water. However, it is interesting to note from the NMR spectra that flocs resulted from the more hydrophobic particles have a slightly higher ratio of free/trapped water, which is also in agreement with their higher specific sediment volume (Figure 6). In other words, although better flocculation can be achieved with more hydrophobic particles, less overall packing density is achieved. This is attributed to the stronger attraction between hydrophobic particles causing a larger viscous force working against the gravitational driving force of better packing of flocs. Interfloc water (bulk water) expulsion is therefore retarded after flocs settle down.

3. Polymer-Flocculated Particles. Polymers are the commonly used flocculants. We have studied dual polymer flocculation with the system Percol−poly(acrylic acid)-

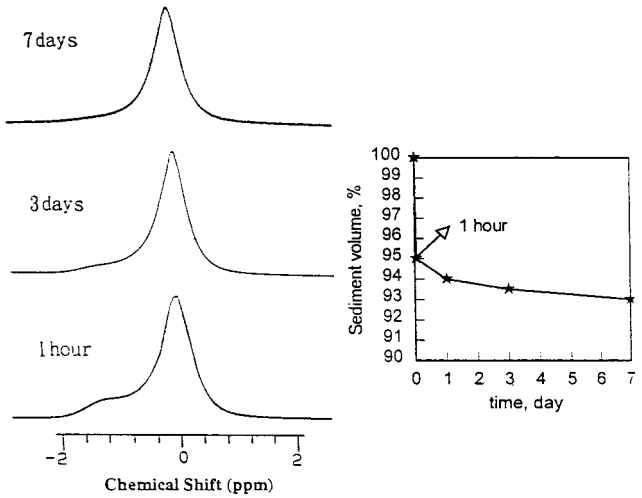

Figure 7. Time effect for flocs induced by dual polymers.

(PAA)−alumina.[40] For this study, 5 ppm of the cationic polymer (Percol) and 5 ppm of the anionic polymer (PAA) were used to produce very good flocculation. In this system, PAA is first adsorbed on alumina and served as the anchor for Percol which bridges the particles together.

NMR spectra were taken at different times after the flocculation. As shown in Figure 7, because of the loose structure of polymer-bridging-induced flocs, the ratio of the trapped-to-bulk water signal is much smaller than that for particles with an adsorbed surfactant and bare particles. The amount of trapped water becomes smaller with time and eventually disappears, with the signal intensity for bulk water staying the same. The disappearance of the trapped water suggests intrafloc water expulsion accompanying polymer rearrangement. This phenomenon occurs more readily with polymer-induced loose flocs where the bulk water removal is hindered by the presence of the polymer.

(40) Fan, A.; Turro, N. J.; Somasundaran, P. Submitted to *Colloids Surf.* **1997**.

Conclusion

The feasibility of using conventional proton NMR spectroscopy for studying floc structure and floc sedimentation is demonstrated. It provides a quick and straightforward method to follow the interfloc and intrafloc water expulsion processes and to examine the floc packing and structure. Some new information was gained on surfactant- and polymer-induced flocs.

Acknowledgment. The authors thank the Environmental Protection Agency (EPA R823301-01-0) and the National Science Foundation for the financial support. They also thank Wei Li in Turro's group for the synthesis of the zeolite samples.

LA980068G